ELSEVIER

Polymer 43 (2002) 2065–2074

polymer

www.elsevier.com/locate/polymer

Crystal polymorphism of poly(butylene-2,6-naphthalate) prepared by thermal treatments

Ming-Yih Ju[a], Jieh-Ming Huang[b], Feng-Chih Chang[a,*]

[a]*Institute of Applied Chemistry, National Chiao-Tung University, Hsinchu 30050, Taiwan, ROC*
[b]*Department of Chemical Engineering, Van Nung Institute of Technology, Chungli, Taiwan, ROC*

Received 13 September 2001; received in revised form 26 November 2001; accepted 17 December 2001

Abstract

The crystal polymorphisms of the poly(butylene-2,6-naphthalate) (PBN) prepared by various thermal treatments in bulk state were investigated. Crystalline forms obtained from different thermal treatments were characterized using wide-angle X-ray diffraction (WAXD) measurements. The α-form crystal is obtained by annealing the quenched PBN sample in the solid state or by crystallizing from the static melt at a relatively lower temperature ($T_C < 205$ °C). On the other hand, an exclusive β-form crystal is generated through unique thermal treatment by non-isothermal crystallization at a cooling rate of 0.1 °C min^{-1} from 280 to 25 °C. Additionally, both α- and β-form crystals appear in the sample melt-crystallized at a relatively higher temperature, and the relative ratio of the α- and β-forms depends on the predetermined crystallization temperature. In this study, it was found that the crystalline form transition never occurs in the solid state. Optical microscopic observations indicate that the α-form crystal exhibits a typical spherulite morphology, while the β-form crystal displays a dendritic spherulite morphology due to the extremely slow spherulite growth rate. Fourier transform infrared spectroscopy was used to examine the crystal structures of both α- and β-forms of the PBN. It is proposed that the main difference between these two crystal structures of PBN prepared by different thermal treatments lies in the packing efficiency of the crystal chains, rather than in the conformation change of the glycol residue, with the β-form possessing tighter packing efficiency than the α-form.

Keywords: Poly(butylene-2,6-naphthalate); Polymorphism; Crystal structure

1. Introduction

The crystal properties of polymers with similar molecular structures, such as poly(*m*-methylene terephthalate) polymers, have attracted considerable interest. The crystallization behaviors and crystal structures of poly(ethylene terephthalate) (PET), poly(butylene terephthalate) (PBT) and poly(ethylene-2,6-naphthalate) (PEN) have been studied extensively [1–10]. For PBT and PEN, it is well known that two different crystal modifications can be formed in the crystalline phase. By applying proper crystallization conditions, such as mechanical deformation or thermal treatment, different modifications will turn up in the crystalline phase [4–10].

The existence of two crystal modifications of the poly(butylene-2,6-naphthalate) (PBN) was first reported by Watanabe [11]. Watanabe found that the PBN film underwent a crystalline phase transformation from the α-form to the β-form while it was uniaxially drawn, which is similar to the case of PBT [4–6,14–17]. Furthermore, he found that the unit cell of the α-form was triclinic, with the following parameters: $a = 0.487$ nm, $b = 0.622$ nm, $c = 1.436$ nm (fiber axis), $\alpha = 100.78°$, $\beta = 126.90°$, $\gamma = 97.93°$, and theoretical density $\rho = 1.36$ g cm^{-3}. Recently, Koyano et al. [12] were able to prepare the exclusive β-form of PBN by stretching the PBN film up to a much higher aspect ratio and described the cell dimensions of the β-form. Their work suggested that the unit cell of the β-form was also triclinic, with parameters $a = 0.455$ nm, $b = 0.643$ nm, $c = 1.531$ nm (fiber axis), $\alpha = 110.1°$, $\beta = 121.1°$, $\gamma = 100.6°$, and theoretical density $\rho = 1.39$ g cm^{-3}. For both the α- and β-forms, each unit cell was found to contain one repeat unit. Additionally, the chain conformations and crystal structures of the α- and β-forms prepared via such a mechanical deformation method were also analyzed in detail by Koyano et al. [12]. They proposed that the main difference between the crystal structures of the α- and β-forms of PBN prepared by mechanical deformation lies in the conformational change of the glycol residue: $\overline{SG}TGS$ for the α-form and TST$\bar{S}$T for

* Corresponding author. Tel.: +886-3-5712121x56502; fax: +886-3-5723764.
E-mail address: changfc@cc.nctu.edu.tw (F.-C. Chang).

0032-3861/02/$ - see front matter
PII: S0032-3861(01)00808-4

the β-form. That is, the molecular chain in the β-form is more extended than that in the α-form. A similar conclusion was also stated by Yamanobe et al. [13], who have studied the influence of external stress on the conformation change of PBN molecules by solid-state ^{13}C-NMR. Accordingly, it was suggested that both the crystal structures of the α- and β-forms of PBN are similar to those of the α and β-forms of PBT [5], respectively.

Since the PBN possesses a molecular structure similar to that of PEN, it can be expected that the crystallization behavior of PBN would somewhat resemble that of PEN. Buchner et al. [8] have reported that PEN can crystallize into two different crystalline forms, depending on the conducted thermal treatment. The α-form is generated by annealing amorphous PEN in the solid state, while the β-form can be obtained, along with a small amount of the α-form, by crystallization from the melt at a high temperature. Furthermore, it was also shown that for PEN the changes in crystalline form never occurs in the solid state, and that the β-form is not only more stable than the α-form, but also more difficult to generate [8]. Recently, Chiba et al. [18] reported that both α- and β-forms of PBN were generated simultaneously by isothermal crystallization at 230 °C from the static melt. A similar result was also observed in the bulk sample crystallized isothermally from the melt at 220 °C as presented in our previous study [19]. In addition, Tsubakihara and Yasuniwa [20] have also reported their study on the exclusive formation of the β-form of PBN by non-isothermal crystallization. These findings reveal that the exclusive β-form of PBN can be obtained through certain thermal treatment.

In an earlier work [19], we have studied the multiple melting behavior of PBN crystallized under different thermal treatments. As a further study, this present work aims to investigate the effect of thermal treatments on the crystal polymorphisms of the non-oriented PBN in the bulk and static states. The crystalline forms in the heat-treated samples were characterized by wide-angle X-ray diffraction (WAXD) measurements. Furthermore, infrared spectroscopy, a powerful, non-destructive and fast means of detailing conformational and structural changes in polymer chains, was applied to study the structural characterization of the crystalline forms of PBN.

2. Experimental

2.1. Material and sample preparation

Additive-free PBN pellets with an inherent viscosity of 0.62 were kindly provided by Shinkong Synthetic Fibers Inc. of Taiwan. The mass loss is less than 5% at 300 °C after 3 h under a nitrogen atmosphere, measured with a thermogravimetric analyzer from Perkin–Elmer, TGA-7. All the crystallization and annealing processes were conducted in the cell of the differential scanning calorimeter (DSC) with an accurate temperature control (±0.1 °C). The bulk PBN pellets were packed in the DSC pan and then subjected to crystallization procedures from both melt and solid states, non-isothermally and isothermally. For the non-isothermal crystallization, the PBN pellets were preheated at 280 °C for 10 min, then cooled to 25 °C using various cooling rates. For the isothermal melt-crystallization, the PBN was preheated at 280 °C for 10 min, cooled down to the predetermined temperature at a rate of 100 °C min^{-1}, maintained isothermally for the desired duration, and then quenched in liquid nitrogen to terminate the crystallization process. Finally, for the cold-crystallization, the liquid nitrogen-quenched sample (from 280 °C for 10 min) was annealed at a predetermined temperature for 3 h in the solid state, followed by quenching in liquid nitrogen to terminate the annealing process. Detailed crystallization conditions will be described in Section 3. The PBN samples thus prepared by various thermal treatments, as well as the as-received PBN pellets, were cryogenically pulverized at the liquid nitrogen temperature in a small type blender for further examinations.

2.2. Apparatus

A DSC instrument from Du Pont (DSC 2010) equipped with a liquid nitrogen-cooling accessory was used to conduct various crystallization conditions. A nitrogen-purge flow at 25 ml min^{-1} was used throughout the experiment to minimize possible oxidation or degradation. Prior to the experiment, a two-point temperature calibration was performed using the indium and tin standards by heating at 10 °C min^{-1}.

The WAXD intensity profiles of the heat-treated samples in the powder form were obtained at ambient conditions using the Mac Science 18 kW rotating anode X-ray generator (M18XHF) with Cu Kα radiation (50 kV, 200 mA, $\lambda = 0.154$ nm). The incident light was monochromatized by a Gr(111) crystal to eliminate Cu Kβ contamination. The scattering angle was measured from 5 to 40° at a scanning rate of 2° min^{-1}. The 2θ peak positions were observed from the resultant profiles, and the corresponding d-spacing values were calculated by Bragg's law

$$\lambda = 2d \sin \theta$$

The crystal morphology of the PBN was examined using a polarized optical microscope (Leitz LABORLUX 12POLS) equipped with a heating stage (Linkam THMS-600) and a temperature control system (Linkam TP-92). The as-received PBN in the powder form was melted on a glass slide at 280 °C at the heating stage, pressed with a piece of cover glass to form a thin film, and then subjected to thermal treatment described earlier. The morphology between the crossed polarizers was viewed and photographed.

Infrared spectroscopic measurements were carried out as follows. The powdered heat-treated sample was thoroughly mixed with the KBr powder (PBN/KBr = 20/80 by weight)

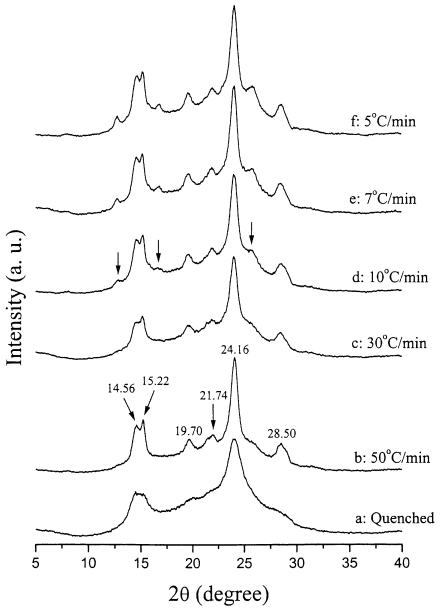

Fig. 1. WAXD intensity profiles of the non-isothermally crystallized PBN prepared by high cooling rates.

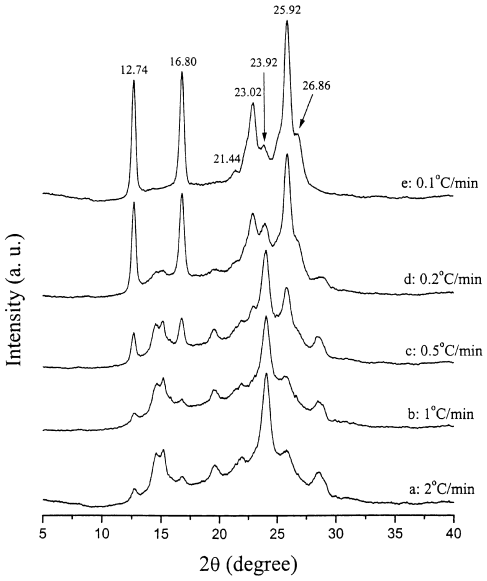

Fig. 2. WAXD intensity profiles of the non-isothermally crystallized PBN prepared by low cooling rates.

to ensure uniform dispersal of the small PBN particles in the KBr matrix. This mixture was subsequently compression-molded into disk under a pressure of 600 psi. The infrared spectrum was examined at room temperature using a Nicolet AVATAR 320 FTIR spectrometer ranging from 400 to 4000 cm^{-1} with a resolution of 1.0 cm^{-1}. The frequency scale was internally calibrated using a He–Ne laser, and 32 scans were single-averaged to reduce noise. All FTIR spectra were obtained under a nitrogen atmosphere to minimize the effects of CO_2 and moisture.

3. Results and discussion

3.1. Crystalline forms in the non-isothermally crystallized PBN samples

Figs. 1 and 2 shows the WAXD intensity profiles of the non-isothermally crystallized PBN samples that were prepared with high and low cooling rates, respectively. Two diffraction peaks at ca. $2\theta = 15$ and 24° can be discerned easily on the profile of the quenched PBN (Fig. 1(a)), indicating that the PBN crystallizes so rapidly that certain quantity of crystals generates even if the sample is quenched immediately from the melt. This result also illustrates the difficulty in measuring the glass transition temperature of PBN via DSC as discussed in our previous report [19]. On the profile of the sample cooled down at a rate of 50 °C min^{-1}, as shown in Fig. 1(b), the peaks can be distinguished clearly, and the characteristic peaks are assigned to the reflections of the α-crystalline form of PBN. This profile is consistent with the results of α-form reported in Refs. [18–21], in which the PBN sample was prepared by isothermal crystallization at 200 °C from the melt. When the cooling rate is decreased to 10 °C min^{-1}, several small peaks emerge on the profile at $2\theta = 12.88$, 16.64 and 25.86° as indicated by the arrows in Fig. 1(d). The intensities of these three peaks increase progressively with decreasing cooling rate, while the intensities of those peaks associated with the α-form gradually decrease, especially when the cooling rate is below 1 °C min^{-1} as shown in Fig. 2. Ultimately, when the cooling rate is further decreased to 0.1 °C min^{-1}, the non-isothermally crystallized PBN exhibits a thoroughly different profile from that of the α-form, as shown in Fig. 2(e). The *d*-spacings of these two different crystalline forms of PBN prepared by non-isothermal crystallization at 50 and 0.1 °C min^{-1} in this work, as well as those calculated using the reported cell parameters of the α- and β-forms of PBN [11,12] and the equations for a triclinic unit cell [22], are listed in Table 1. It can be seen in Table 1 that the observed *d*-spacings of the crystalline form prepared at a cooling rate of 50 °C min^{-1} are in good agreement with the calculated values of the α-form. The *d*-spacings of the crystalline form prepared at 0.1 °C min^{-1} are mostly consistent with the calculated values of the β-form except the substantial deviation for the $(0\bar{1}1)$ and (010) planes. This *d*-spacing deviation for the $(0\bar{1}1)$ and (010) planes can be attributed to the cell parameters of the β-form determined in the highly stretched state, which has also been reported by Chiba et al. [18]. Because of the substantial *d*-spacing deviation of the $(0\bar{1}1)$ and (010) planes, the crystalline form shown in Fig. 2(e) prepared at an extremely low cooling rate (0.1 °C min^{-1}) is designated as β′-form to differentiate from the β-form prepared by highly mechanical deformation. Furthermore, according to the variation of the crystal polymorphism with the conducted cooling rates shown in

Table 1
d-spacings of the observed crystalline forms of PBN compared with those of the α- and β-form crystals calculated according to the reported cell parameters of PBN [11,12]

Crystal form	Lattice planes	d_{cal} (nm)	d_{obs} (nm)	RI[a]
α	$(0\bar{1}1)$	0.603	0.608	m
	(010)	0.579	0.582	m
	(011)	0.450	0.450	mw
	$(\bar{1}11)$	0.406	0.409	mw
	(100)	0.369	0.368	s
	$(1\bar{1}0)$	0.369		
	$(1\bar{1}1)$	0.311	0.313	mw
β	$(0\bar{1}1)$	0.631	0.694	s
	(010)	0.539	0.524	s
	$(\bar{1}03)$	0.416	0.414	w
	$(1\bar{1}0)$	0.381	0.386	m
	(003)	0.373	0.372	w
	(100)	0.348	0.343	s
	$(1\bar{1}1)$	0.330	0.332	w

[a] Relative intensity observed on the diffraction profiles.

Figs. 1 and 2, it can be concluded that the α-form is kinetically favorable while the β′-form is thermodynamically favorable.

3.2. Crystalline forms in the isothermally crystallized PBN samples

WAXD profiles of the PBN crystallized isothermally at 220 and 200 °C for various durations from the static melt are shown in Fig. 3(a) and (b), respectively. Regardless of crystallization duration, both α- and β′-forms are present in samples crystallized at 220 °C, while only the α-form appears in samples crystallized at 200 °C. In Fig. 3(a), those peaks associated with the α-form sharpen up to the crystallization time of 60 min, indicating that crystallization is in progress. When crystallization time increases beyond 60 min, the profile does not change noticeably. Meanwhile, the diffraction profiles of samples crystallized at 200 °C exhibit no apparent variation with crystallization time, as shown in Fig. 3(b). These profiles indicate that the crystalline form of PBN does not change at a single crystallization temperature (T_C). Fig. 4 shows the WAXD profiles of PBN crystallized isothermally at different temperatures from the melt for 3 h, where the effect of T_C on the crystal polymorphism of PBN is demonstrated. Although the true fraction of α- and β′-forms in the crystalline phase cannot be quantified, the change in the relative ratio of these two forms can be obtained by comparing the intensities of the peaks associated with the α- and β′-forms, respectively. As the conducted T_C is decreased, the intensity of the peaks associated with the β′-form decreases while that of the peaks associated with the α-form increase as shown in Fig. 4, indicating the decreasing fraction of the β′-form in the crystalline phase. Finally, only the α-form is detected when T_C is below 205 °C.

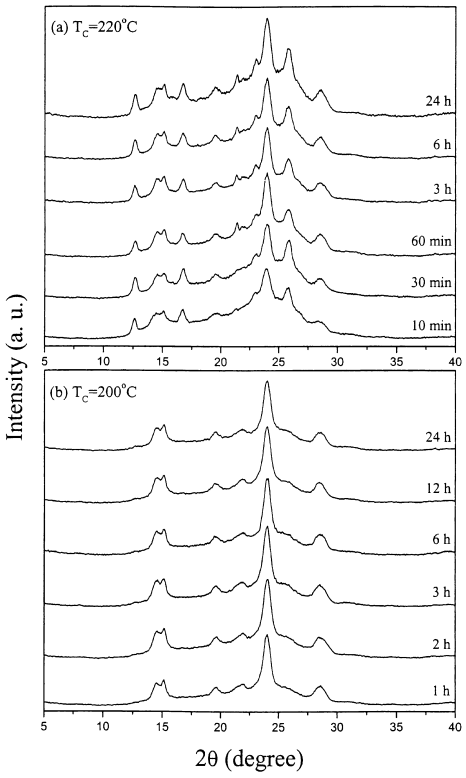

Fig. 3. WAXD intensity profiles of PBN crystallized isothermally at (a) 220 °C and (b) 200 °C from the melt for various durations as indicated.

Fig. 5 shows the WAXD profiles of the cold-crystallized PBN samples that were annealed isothermally at different temperatures for 3 h in the solid state. Only the α-form is detected in these cold-crystallized samples, even if the annealing temperature is raised to 230 °C. Since a totally amorphous PBN cannot be obtained even by quenching in

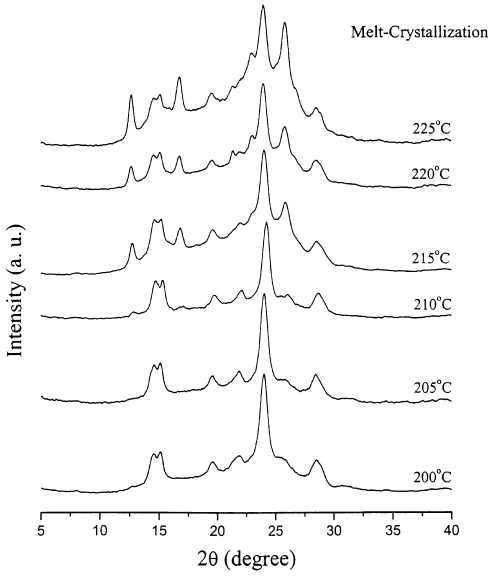

Fig. 4. WAXD intensity profiles of PBN crystallized isothermally at different temperatures from the melt for 3 h.

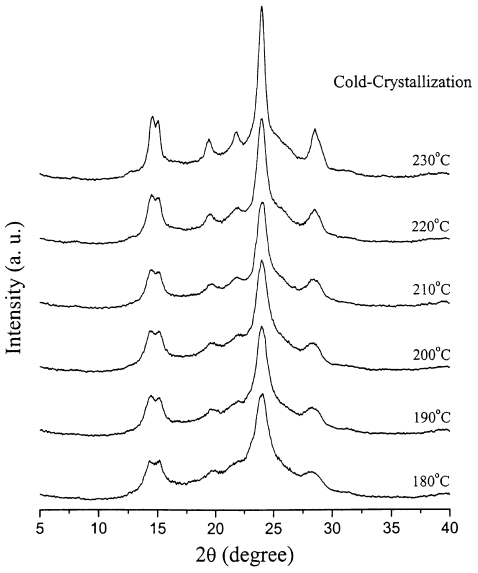

Fig. 5. WAXD intensity profiles of the cold-crystallized PBN samples that were annealed isothermally at different temperatures in the solid state for 3 h.

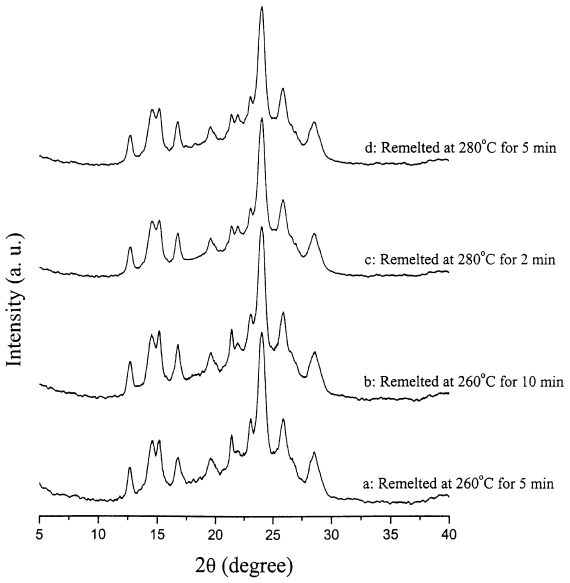

Fig. 7. WAXD intensity profiles of the PBN samples originally in the β′-form that were subjected to different remelting procedures and then crystallized at 200 °C for 3 h.

liquid nitrogen, and thus the evolution of the crystal polymorphism would be limited since the crystalline entities associated with the α-form are already present (Fig. 1(a)). The peaks grow and sharpen as the annealing temperature is raised, illustrating the increased crystallinity and perfection of crystals.

3.3. Thermal treatments on the β′-form of PBN

In previous studies [18,19], PBN samples have been step-crystallized between two temperatures, e.g. 220 and 200 °C, to inspect the crystalline form change during the step-crystallization process. It was observed that the crystalline form of PBN is determined by the initial T_C, and the annealing treatment conducted at other temperatures thereafter does not alter the existing form. Since the exclusive β′-form of PBN can be obtained by unique thermal treatment as described earlier, it is interesting to know the influence of further thermal treatment on this thermally prepared β′-form. Fig. 6 shows the WAXD profile of the annealed PBN sample that was originally in the β′-form. This β′-form sample was annealed at 220 °C for 12 h in the solid state. Evidently, the crystalline form detected in this annealed sample remains in the β′-form. It also can be seen in Fig. 6 that after annealing the peaks at $2\theta = 21.44$, 23.92 and 26.86° become sharper than those shown in Fig. 2(e). Additionally, a shoulder at $2\theta = 22.28°$ and a peak at $2\theta = 25.10°$ emerge on the profile of this annealed sample, as indicated by arrows in Fig. 6. These shoulder and peak can be ascribed to reflections corresponding to the $(\bar{1}11)$ ($d_{cal} = 0.402$ nm) and $(\bar{1}04)$ ($d_{cal} = 0.351$ nm) planes, respectively. Fig. 6 shows that the thermally prepared β′-form crystals of PBN become more complete and perfect during the annealing process performed at 220 °C. Consequently, based on the results presented herein and those reported previously [19], it can be concluded that the PBN crystalline form change never occurs in the solid state.

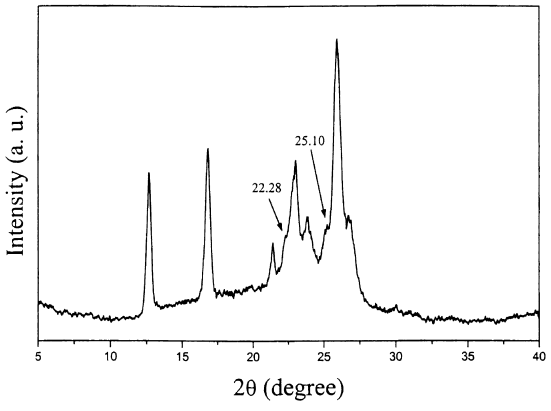

Fig. 6. WAXD intensity profile of the annealed PBN sample that was originally in the β′-form. The sample was prepared by non-isothermal crystallization at a cooling rate of 0.1 °C min^{-1} from the melt and then annealed at 220 °C in the solid state for 12 h.

In order to examine the stability of the β′-form after remelting, PBN samples originally in the β′-form were remelted at 260 and 280 °C separately for various durations and subsequently crystallized at 200 °C for 3 h. Remelting temperatures of 260 and 280 °C were chosen because the equilibrium melting temperature (T_m^0) of PBN has been determined at 276 °C [19]. The resultant WAXD profiles are shown in Fig. 7. Both α- and β′-forms are clearly detected in these remelted samples after crystallization at 200 °C. Notably, only the α-form was obtained at $T_C = 200$ °C (Fig. 3(b)) when samples were prepared

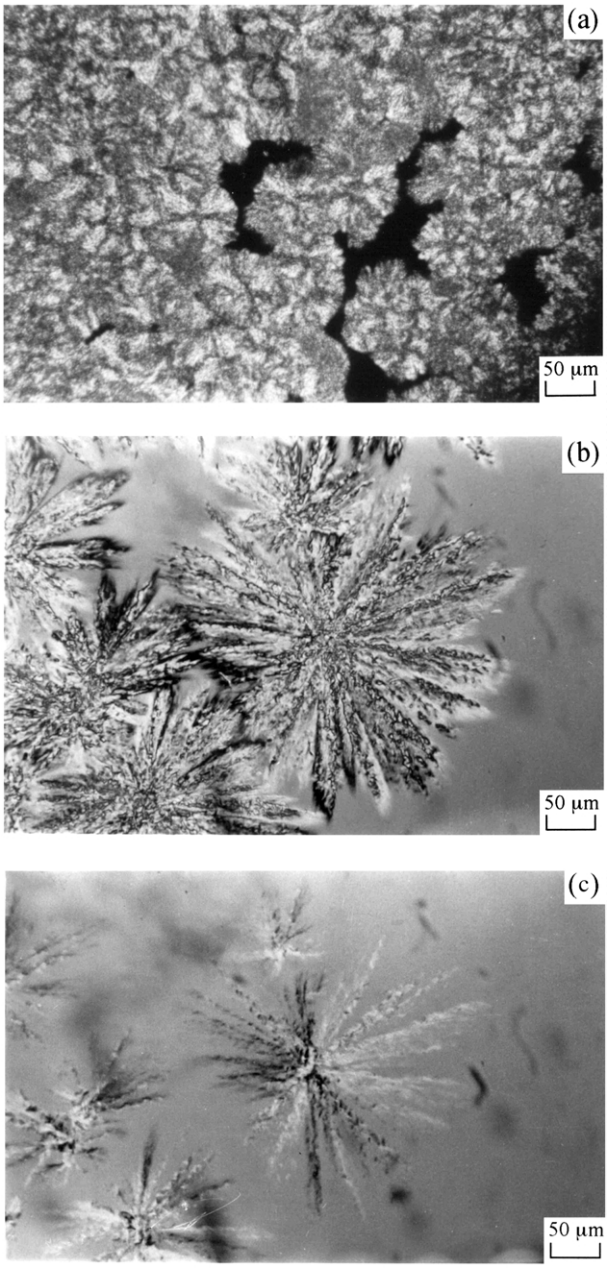

Fig. 8. Cross-polarized optical micrographs of PBN: (a) α-form crystal; (b) β′-form crystal; (c) the melting of the β′-form crystal obtained by (b) using a heating rate of 10 °C min^{-1}.

from the raw material, as discussed in Section 3.2. Furthermore, regardless of remelting temperature and duration, these profiles exhibit no obvious difference. In general, molecular chains are supposed to be in a random state when a crystalline polymer is heated up beyond its own T_m^0. The WAXD profiles shown in Fig. 7, however, reveals that some of the PBN molecules remain in an ordered structure after remelting. A certain fraction of the β′-form is generated during the later crystallization process at 200 °C, even though the conducted remelting temperature is higher than the T_m^0 of PBN. This result may also lead to the inference that the β′-form crystals may not be completely melted at 280 °C. That means, the thermally prepared β′-form crystal of PBN may possess an equilibrium melting point higher than 276 °C. Experiment is performed to verify this inference.

3.4. Optical microscopic observation

Fig. 8 shows the cross-polarized optical microscopic observations on the PBN samples in α- and β′-forms, and on the melting of the β′-form crystal by heating at a rate of 10 °C min^{-1}. The α- and β′-form samples were prepared by isothermal and non-isothermal crystallization from the melt, respectively, at 200 °C and at a cooling rate of 0.1 °C min^{-1}. Micrographs were taken as the spherulite growth approach their final stage. The α-form crystal of PBN displays a typical morphology of spherulites, as shown in Fig. 8(a). Meanwhile, in Fig. 8(b), the β′-form crystal exhibits a morphology obviously different from that of the α-form. The textures within the β′-form spherulites appear to grow radially and almost individually from the center, resulting in a dendritic spherulite morphology [22]. This unusual morphology originates from the extremely slow spherulite growth rate caused by slow cooling, allowing texture growth to reach the most thermodynamically stable state during the crystallization process. During the melting of the β′-form crystal, as shown in Fig. 8(c), the secondary growth within the spherulite disappeared first, allowing the skeleton to be clearly discerned. In addition, Fig. 8(a) and (b) shows that the β′-form spherulites can grow significantly larger than those of the α-form, and that the numbers of the β′-form spherulites are fewer than the α-form spherulites.

3.5. FTIR spectroscopy

Studies on the infrared spectra of PBN are surprisingly rare in literature. Ouchi et al. [23] have reported the complete band assignments for PBN, but the PBN was not the main subject of their work. Chiba et al. [18] conducted in situ FTIR measurements to study the crystallization kinetics of PBN during melt-crystallization, and reported the band changes associated with the crystalline phase. In the case of PBT, the butylene glycol residue is generally believed to adopt contracted and extended conformations in the α- and β-forms, respectively, as evidenced by X-ray and infrared spectroscopic investigations [5,6,14,15]. In the infrared spectra [6,14,15], the significant changes occur in the methylene rocking region between 900 and 1000 cm^{-1}, while between 1300 and 1550 cm^{-1} the methylene bending region also exhibits good sensitivity. However, investigations on the structure of the α- and β-forms of PBT have caused a controversy over the structure of the α-form. Hall and Pass [14] suggested that changes in the terephthalate residue might occur related to the orientation of the phenylene/carbonyl bonds and the planarity of the residue as a whole. More detailed evidence regarding the chemical environment of the α- and β-forms was presented by Gomez

et al. [17], who employed the high-resolution solid-state ^{13}C-NMR measurements to inspect the molecular structure of PBT. The NMR results for the β-form of PBT are consistent with an almost fully extended molecular conformation. However, the NMR results for the α-form did not agree with any of the previously proposed crystal structures, and suggested that the conformation and orientation of the glycol residue remain essentially unchanged in the strain-induced transformation from the α- to β-form. That is, the glycol residue adopts the all *trans* conformation in both the α- and β-crystalline forms. Additionally, the reported NMR results [16,17] also suggest that changes in the conformation of the terephthalate residue must accompany the crystalline form transition of PBT. Although the NMR measurements indicate the likely conformation of the terephthalate residue, the infrared spectra exhibit no similar results. In the case of PEN, infrared spectroscopic investigation [10] reveals that both the bands associated with the naphthalene ring vibrations and the vibrations of the ethylene glycol residue are influenced by the crystallization of PEN. This observation suggests that the conformation change of PEN occurs simultaneously in ethylene glycol and naphthalate residues during crystallization. Guo and Zachmann [9] have studied the α- and β-crystal structures of PEN using high-resolution solid-state ^{13}C-NMR spectroscopy. They found that a significant chemical shift difference between the spectra of the two crystalline forms occurs in the resonances of the protonated naphthalene ring carbons, and they attributed this result to different chain conformation and packing efficiency. Based on the above descriptions of PBT and PEN, the conformation changes in butylene glycol and naphthalate residues must be considered as a whole for the semi-crystalline PBN.

The infrared spectra of semi-crystalline PBN samples in α- and β′-forms are shown in Figs. 9–12. The spectrum of the quenched PBN sample is also displayed as a comparison since a totally amorphous sample cannot be obtained in bulk. Table 2 lists the observed frequencies in the spectra of the quenched, α- and β′-form samples, along with the tentative band assignments. As discussed earlier, vibration modes in the infrared spectra of PBN can be classified into bands associated with the butylene glycol residue and the naphthalene ring separately. These two units are connected by a C=O group, and thus the C=O stretching vibration should be affected by both units and vice versa. Consequently, the differences of the band associated with the C=O stretching vibration in α- and β′-forms are examined first. The C=O stretching vibration appears at 1718 cm^{-1} in the α-form and at 1713 cm^{-1} in the β′-form as shown in Fig. 9. A similar band shift for the C=O group in the crystalline phase of PEN has also been reported [10] in relative to the conjugation between the C=O group and the naphthalene ring. The greater coplanarity between the C=O group and the naphthalene ring can induce stronger conjugation, resulting in a downward shift in the wavenumber for the C=O group. The observed lower wavenumber of the C=O group thus suggests greater planarity between the C=O group and the naphthalene ring in the β′-form. Furthermore, the planarity appears to influence not only the C=O group but also the whole ester group (–CO–O–). In Fig. 10(b), bands at 1281 and 1260 cm^{-1} in the α-form can be assigned to the =C–O stretching vibration, with partial contribution from the aromatic ring vibration. These two bands shift to lower wavenumber at 1278 and 1256 cm^{-1} in the β′-form as shown in Fig. 10(c), indicating the lower bonding energy of =C–O. In contrast, the bands at 1084 and 1044 cm^{-1} in the α-form, which can be assigned to the O–CH_2 stretching vibration in the

Table 2
IR band assignments of PBN in the quenched, α-form and β′-form samples

Quenched	α-form	β′-form	Assignment[a]
1935 m	1936 m	1935 m	
1823 vw	1824 vw	1825 w	
1785 w	1785 vw	1788 vw	
1717 s	1718 s	1713 s	ν (C=O)
1635 w	1635 w		
1603 m	1602 m	1602 m	Aromatic ring vibration
1502 m	1502 m	1502 m	Aromatic ring vibration
1469 m	1469 m	1470 m	δ (CH_2) *trans*
1448 w	1447 w	1449 w	δ (CH_2) *gauche*
1395 m	1396 m	1402 m	Aromatic ring vibration
1370 sh	1370 w	1375 vw	γ_w (CH_2) *gauche*, split in β′-form
		1369 vw	
1339 m	1339 m	1338 m	γ_w (CH_2) *trans*
1280 m	1281 m	1278 m	ν (=C–O) + aromatic
1260 w	1260 m	1256 m	ν (=C–O) + aromatic
1217 w	1217 w	1218 vw	Aromatic ring vibration
1183 m	1182 m	1182 s	Naphthalene ring vibration
1128 m	1130 m	1130 m	Naphthalene ring vibration
1084 m	1084 m	1087 m	ν_s (O–C) *gauche*
1042 m	1044 m	1052 m	ν_a (O–C) *gauche*
994 w	994 w	994 w	Vibration of *trans* glycol segments
960 vw	962 w	964 m	
943 w	945 w	948 vw	
914 m	914 m	914 m	δ (aromatic CH out-of-plane vibration)
822 m	821 m	826 vw	γ_r (CH_2), split in β′-form
		817 m	
794 m	794 m	793 m	γ_r (C=O) + δ (CCO)
766 S	766 s	766 s	δ (aromatic CH out-of-plane vibration)
741 sh	741 sh	742 sh	
641 m	641 m	640 m	δ (COC)
623 m	622 m	621 w	
556 w	558 w	557 m	Increase in β′-form
535 w	536 w	536 w	Decrease in β′-form
523 w	523 w	522 w	Decrease in β′-form
473 s	473 s	475 s	δ (aromatic CH out-of-plane vibration)
449 w	451 sh		
423 w	423 m		
403 w	403 m	403 w	

[a] ν: stretching, the subscripts 's' and 'a' represent symmetric and anti-symmetric modes, respectively; δ: bending; γ_w: wagging; γ_r: rocking.

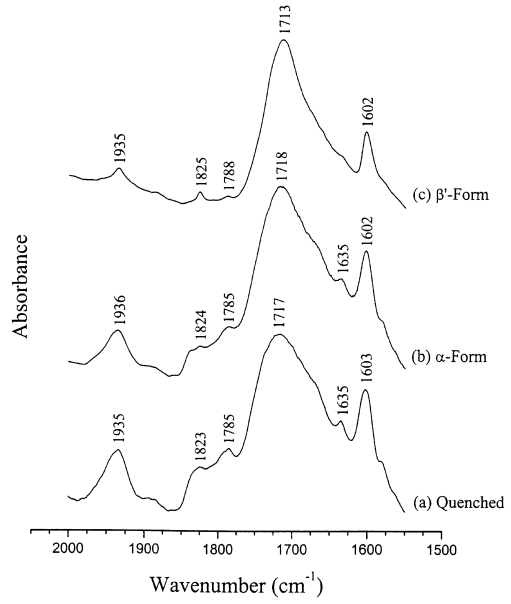

Fig. 9. Infrared spectra of PBN in the region of 1550–2000 cm^{-1}: (a) quenched sample; (b) α-form and (c) β′-form.

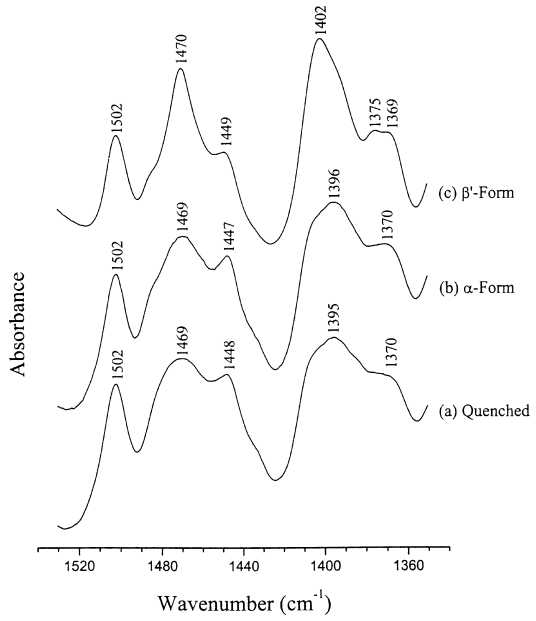

Fig. 11. Infrared spectra of PBN in the region of 1350–1550 cm^{-1}: (a) quenched sample; (b) α-form and (c) β′-form.

symmetric and antisymmetric modes, respectively, shift upward to 1087 and 1052 cm^{-1} in the β′-form (Fig. 10(b) and (c)). These changes in stretching vibrations of the ester group can be attributed to the stronger conjugation in the β′-form. Moreover, the ester group may adopt a different arrangement in the β′-form due to its tighter chain packing in the crystalline phase.

Major bands associated with the naphthalene ring vibration appear in the regions of 1100–1300 and 1400–1600 cm^{-1}. The bands at 914, 766 and 473 cm^{-1} are assigned to the aromatic CH out-of-plane vibration. Chiba et al. [18] assigned the 914 cm^{-1} band to the CH_2 rocking vibration and found that this band splits into two bands after thermal treatment. However, this 914 cm^{-1} band exhibits no apparent change with thermal treatment herein (Fig. 12), and thus we favor the assignment of Ouchi et al. [23]. By digital subtraction of the amorphous spectrum from the semi-crystalline spectra, Vasanthan and Salem [10] found that the bands associated with the naphthalene in-plane vibration of PEN show a substantial shift in different

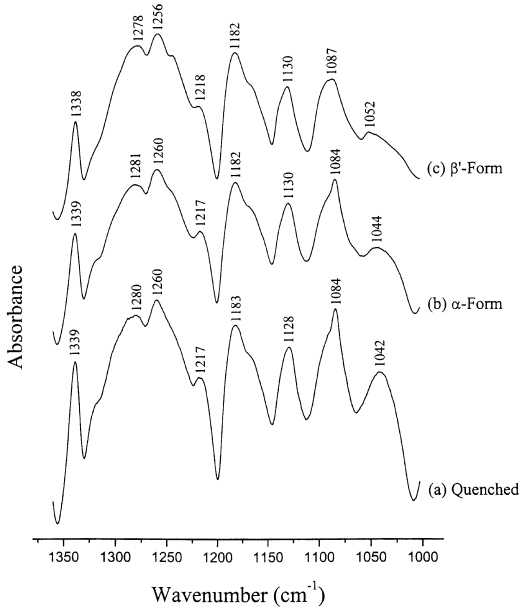

Fig. 10. Infrared spectra of PBN in the region of 1000–1360 cm^{-1}: (a) quenched sample; (b) α-form and (c) β′-form.

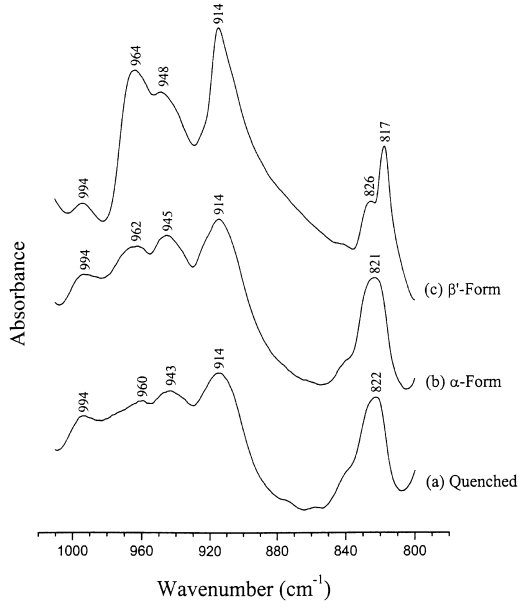

Fig. 12. Infrared spectra of PBN in the region of 780–1020 cm^{-1}: (a) quenched sample; (b) α-form and (c) β′-form.

crystalline forms. Such results suggest that the naphthalene ring adopts a different conformation in each form. However, in the raw spectra of PBN, no similar behavior has been observed between α- and β′-forms. Nevertheless, the band associated with the naphthalene ring vibration appearing at 1396 cm^{-1} in the α-form shifts upward to 1402 cm^{-1} in the β′-form as shown in Fig. 11. Although this phenomenon is still inconclusive as evidence, it reveals that the conformational arrangement of the naphthalene ring differs between α- and β′-forms.

The band at 821 cm^{-1} in the α-form (Fig. 12(b)) is assigned to the CH_2 rocking vibration. In the β′-form, this band splits into two separate bands at 826 and 817 cm^{-1}, as shown in Fig. 12(c). The splitting of the band associated with the CH_2 rocking vibration in the β′-form of PBN is quite different from that in PBT [6,14,15], where a new band appears at a higher wavenumber in the extended β-form and is assigned to the CH_2 rocking vibration in the *trans* mode. Ouchi et al. [23] have found that the band at 821 cm^{-1} appears in all naphthalene-containing polyesters, whereas the new bands form due to crystallization appears only in the case of PEN, and not in other cases. In the case of polyethylene [24], the splitting of the band at 720 cm^{-1} associated with the CH_2 rocking vibration was also observed, and was considered the consequence of the intermolecular interaction in the crystalline state. Therefore, the splitting of the 821 cm^{-1} band strongly suggests that the PBN molecular chains are packed more tightly in the β′-form than in the α-form. Splitting also occurs in the band associated with the CH_2 wagging vibration in the *gauche* mode, which appears at 1370 cm^{-1} in the α-form and splits into two weak bands at 1375 and 1369 cm^{-1} in the β′-form, as shown in Fig. 11. The conformation of the butylene glycol residue of PBN is characterized in the region of 1300–1500 cm^{-1}, where the CH_2 wagging and bending vibrations in the *trans* and *gauche* modes become evident. The band at 1338 cm^{-1} is assigned to the *trans* CH_2 wagging vibration. This same band has also been assigned to the *trans* CH_2 wagging vibration in the amorphous phase for PET [2,23] and PEN [10]. In the case of PEN [10], the band at 1338 cm^{-1} in the amorphous spectrum shifts to 1332 cm^{-1} in the α-form and to 1347 cm^{-1} with a shoulder at 1332 cm^{-1} in the β-form, indicating that the α-form only contains the *gauche* component, while the β-form contains both the *trans* and *gauche* components. In the spectra of the α- and β′-forms of PBN, as shown in Fig. 10, no new band forms in the vicinity of 1338 cm^{-1}, and the band position exhibits no changes. Regarding the bands associated with the *trans* and *gauche* CH_2 bending vibrations that appear at 1470 and 1449 cm^{-1} (Fig. 11), no change is observed in the spectra of the α- and β′-forms of PBN. Besides, the band appearing in the region between 990 and 962 cm^{-1} has been associated with the vibration of the *trans* glycol segments of PBT by Ward and Wilding [6], and hence this study assigns the 994 cm^{-1} band in the same manner. Since the 994 cm^{-1} band exhibits no significant change in position between the spectra of the α- and β′-forms of PBN, the conformations of the glycol residue in these two crystalline forms appear unchanged. Consequently, the glycol residue of PBN adopts a similar conformation in both α- and β′-forms.

Based on the infrared spectroscopic results, it is proposed that the main difference between the thermally prepared α- and β′-crystal structures of PBN lies in the packing efficiency of the crystal chains and not in the conformation change of the glycol residue. Crystal chains in the β′-form are packed more tightly than those in the α-form, and the glycol residue adopts a similar conformation in both the forms. The conformational arrangements of the naphthalene ring differ in these two forms of PBN, and the planarity of the naphthalate residue in the β′-form exceeds that in the α-form. Consequently, the greater planarity provides a better opportunity for higher packing efficiency of the crystal chains. This fact may be also evidenced by the different densities of the crystalline forms, which are 1.36 and 1.39 g cm^{-3} for the α- and β-forms, respectively, [12]. Although previous works have observed the conformation change of the glycol residue between the two crystalline forms of PBN, obviously such a change is caused by the externally applied stress.

4. Conclusions

The crystalline forms and crystal structures of PBN prepared by different thermal treatments in bulk state were studied. The α-form is obtained by annealing the quenched PBN sample in the solid state or by crystallizing from the static melt at a lower temperature ($T_C < 205$ °C). On the other hand, by performing non-isothermal crystallization at an extremely low cooling rate (0.1 °C min^{-1}) from the melt on the static PBN sample, an exclusive β′-form is generated. This thermally prepared β′-form possesses a WAXD profile similar to that of the reported β-form prepared by highly mechanical deformation, except for the substantial *d*-spacing deviation in $(0\bar{1}1)$ and (010) planes. At a higher T_C, both α- and β′-forms are obtained simultaneously, and the relative ratio between the amount of α- and β′-forms is dependent on the predetermined crystallization temperature. Additionally, crystalline form change never occurs in the solid state. The spherulite morphologies of the two forms differ markedly. The α-form crystal exhibits a typical spherulite morphology, while the β′-form crystal possesses a dendritic spherulite morphology due to the extremely slow spherulite growth rate. Finally, based on the infrared spectroscopic results, it is proposed that the main difference between the α- and β′-crystal structures of PBN prepared by thermal treatments lies in the packing efficiency of the crystal chains, rather than in the conformation change of the glycol residue. The crystal chains in the β′-form are more tightly packed than those in the α-form, while the glycol residue adopts a similar conformation in both the forms.

Acknowledgements

The authors thank the Shinkong Synthetic Fibers Inc. for kindly providing the PBN pellets and Dr Hsin-Yih Lee at Synchrotron Radiation Research Center for providing the WAXD instrument.

References

[1] Daubeny RP, Bunn CW, Brown C. J Proc R Soc Lond, Ser A 1954;226:531.
[2] Liang CY, Krimm S. J Mol Spectrosc 1959;3:554.
[3] Liu J, Koenig JL. Anal Chem 1987;59:2609.
[4] Mencik Z. J Polym Sci, Part B: Polym Phys 1975;13:2173.
[5] Yokouchi M, Sakakibara Y, Chatani Y, Hiroyuki T, Tanaka T, Yoda K. Macromolecules 1976;9:266.
[6] Ward IM, Wilding MA. Polymer 1977;18:327.
[7] Mencik Z. Chem Prum 1976;17:78.
[8] Buchner S, Wiswe D, Zachmann HG. Polymer 1989;30:480.
[9] Guo M, Zachmann HG. Macromol Chem Phys 1998;199:1185.
[10] Vasanthan N, Salem DR. Macromolecules 1999;32:6319.
[11] Watanabe H. Kobunshi Ronbunshu 1976;33:299.
[12] Koyano H, Yamamoto Y, Saito Y, Yamanobe T, Komoto T. Polymer 1998;39:4385.
[13] Yamanobe T, Matsuda H, Imai K, Hirata A, Mori S, Komoto T. Polym J 1996;28:177.
[14] Hall IH, Pass MG. Polymer 1976;17:807.
[15] Stambaugh B, Lando JB, Koenig JL. J Polym Sci, Part B: Polym Phys 1979;17:1063.
[16] Davidson IS, Manuel AJ, Ward IM. Polymer 1983;24:30.
[17] Gomez MA, Cozine MH, Tonelli AE. Macromolecules 1988;21:388.
[18] Chiba T, Asai S, Xu W, Sumita M. J Polym Sci, Part B: Polym Phys 1999;37:561.
[19] Ju MY, Chang FC. Polymer 2001;42:5037.
[20] Tsubakihara S, Yasuniwa M. Polym Prepr Jpn 1999;48:4181 (in Japanese).
[21] Lee SC, Yoon KH, Kim JH. Polym J 1997;29:1.
[22] Wunderlich B. Macromolecular physics, vol. 1. New York: Academic Press, 1973. Chapter 3.
[23] Ouchi I, Hosoi M, Shimotsuma S. J Appl Polym Sci 1977;21:3445.
[24] Krimm S, Liang CY, Sutherland GBBM. J Chem Phys 1956;25:549.